# On Asymmetrically Clipped Hybrid FSK-Based Unipolar Modulations: Performance and Frequency-Domain Analysis

Clara Chateigner, Yannis Le Guennec, Laurent Ros, Cyrille Siclet

# On Asymmetrically Clipped Hybrid FSK-Based Unipolar Modulations: Performance and Frequency-Domain Analysis

Clara Chateigner
*Univ. Grenoble Alpes, CNRS*
*Grenoble-INP, GIPSA-Lab*
Grenoble, France
clara.chateigner@gipsa-lab.grenoble-inp.fr

Yannis Le Guennec
*Univ. Grenoble Alpes, CNRS*
*Grenoble-INP, GIPSA-Lab*
Grenoble, France
yannis.le-guennec@gipsa-lab.grenoble-inp.fr

Laurent Ros
*Univ. Grenoble Alpes, CNRS*
*Grenoble-INP, GIPSA-Lab*
Grenoble, France
laurent.ros@gipsa-lab.grenoble-inp.fr

Cyrille Siclet
*Univ. Grenoble Alpes, CNRS*
*Grenoble-INP, GIPSA-Lab*
Grenoble, France
cyrille.siclet@gipsa-lab.grenoble-inp.fr

***Abstract*—Envelope detection, commonly used in visible light communication systems or in some radiofrequency receivers, requires the definition of real and unipolar modulations. With the objective of maximizing the energy efficiency of the modulation for a given spectral efficiency ($\leq$ 1 bit/s/Hz, compatible with low power low data rate applications), a hybrid modulation that merges the elements of non-linear and linear modulations (named as hybrid asymmetrically clipped frequency-shift keying (AC FSK)-based modulation) is investigated. Comparing the performance for different linear (amplitude/phase) modulations, it is shown that the use of phase-shift keying (PSK) with 4 or 8 states for the linear part offers the best spectral efficiency vs energy efficiency trade-off. Moreover, a frequency-domain analysis of the waveforms facilitates the implementation of a low complexity quasi optimal harmonic receiver. Finally, a closed-form expression of power spectral density for AC-FSK-PSK modulation is defined, leading to a relevant definition for signal bandwidth and spectral efficiency.**

***Index Terms*—Unipolar modulations, frequency-shift keying, hybrid modulations, visible light communications.**

## I. Introduction

Wireless communications are major contributors to the carbon footprint of digital technologies. Among emerging wireless techniques, a significant number of communication systems use envelope detection in receivers. For example, photodiodes are used in visible light communications (VLC) [1], and Shottky diodes in millimeter wave (mmW) envelope detectors [2]. Envelope detection requires unipolar and real modulations. Unipolar linear modulations such as pulse-amplitude modulation (PAM) or baseband orthogonal frequency division multiplexing (OFDM) have been widely considered for envelope detection receivers [3], [4]. However, linear modulations are known to exhibit high spectral efficiency to the detriment of energy efficiency [5]. Since some wireless applications are not constrained by spectral efficiency (considering low data rate connectivity in sensor networks, for example), it is relevant to consider modulations with a lower spectral efficiency but higher energy efficiency, with the priority target to decrease the overall power consumption of the wireless communication system. The energy efficiency of unipolar linear modulations is upper bounded by the 2-state modulation case (i.e. on-off-keying (OOK) modulation). Conversely, using non-linear modulations, it is possible to outperform the energy efficiency of the 2-state case by increasing the modulation order. The first non-linear modulation, which has been extensively studied for optical wireless communications (OWC), is pulse-position modulation (PPM) [6]. Unfortunately, PPM has some severe limitations, such as strong peak-to-average power ratio, synchronization issues and strong multi-path channel impact. Unipolar frequency-shift keying (FSK) circumvents the limitations of PPM. In [7], an asymmetric FSK (AFSK) technique is presented for OWC, but only 2 modulation states are considered for performance evaluation. In [8], an asymmetrically clipped (AC) hybrid frequency- and phase-shift keying (FPSK) modulation scheme, renamed here AC-FSK-PSK, is proposed and shows higher energy efficiency than conventional linear modulations. Indeed, as previously seen in hybrid modulations literature [9], [10], the aim of combining a non-linear modulation such as FSK with a linear modulation (PSK here) is to take advantage of both modulations, respectively in terms of energy efficiency and spectral efficiency. Still in [8], a low-complexity harmonic receiver is proposed for AC-FSK-PSK, based on frequency-domain (FD) cross-correlation which necessitates an off-line computation of FD waveforms. Against the given background, the contributions of this article are as follows:

1) We propose a generalization of AC hybrid FSK-based modulations (in section II) to evaluate and compare the performance for different possible linear "phase/amplitude" modulation alphabets (in section IV). This highlights the superior performance of PSK alphabets over alternatives.
2) We derive a closed-form expression of the dictionary waveforms in FD (in section III), that permits to justify the frequency grid chosen for the modulation part, and to theoretically elucidate the harmonic receiver of [8], avoiding off-line computation of the components.
3) We derive a closed-form expression of the power spectral density (PSD) of hybrid AC-FSK-PSK (in section V), leading to more accurate evaluations of the signal bandwidth and related spectral efficiency.

## II. AC HYBRID FSK-BASED MODULATIONS

### A. Analog waveforms

In AC hybrid FSK-based modulations, symbols are built from a $2M_\perp$-FSK dictionary, for which only the $M_\perp$ odd frequencies are considered and modulated by a linear amplitude and phase modulation, i.e. $M_L$ complex elementary symbols expressed as $A_i e^{j\phi_i}$, $A_i$ and $\phi_i \in \mathbb{R}$ and $A_i \geq 0$. To ensure a positive-valued signal, the hybrid linear/FSK symbol is clipped to force to zero negative samples. The analog waveform from the AC hybrid FSK-based dictionary of frequency index $m \in \{1,3,\cdots,2M_\perp-1\}$ and linear modulation $A_i e^{j\phi_i}$, $i \in \{0,1,\cdots,M_L-1\}$, is expressed as:

$$g_{m,i}(t) = \text{Clip}\{A_i \cos(2\pi m \Delta f\ t + \phi_i)\} \cdot \Pi_{[0;T_s[}(t), \quad (1)$$

where Clip is the ramp function: $\text{Clip}(x)=x$ if $x \geq 0$ and $\text{Clip}(x)=0$ otherwise. The frequency grid of the initial $2M_\perp$-FSK modulation uses the subcarrier spacing $\Delta f = \frac{1}{T_s}$, and $\Pi_{[0;T_s[}$ is the rectangular function from 0 to $T_s$ of amplitude 1. The choice to keep only odd-indexed frequencies (spaced finally by $2\Delta f$) was inspired in [8] by ACO-OFDM framework [4]. Actually, as it will be demonstrated in part III, the distortion induced by the clipping of a hybrid FSK-based symbol (with an odd-indexed frequency carrier) falls into the even-indexed frequency carriers. The size of the AC hybrid FSK-based modulation dictionary is $M = M_\perp M_L$.

Against the work of [8], various linear modulations are considered here for the AC hybrid FSK-based modulation, in order to find out the one achieving the best trade-off between energy efficiency and spectral efficiency: pulse-amplitude modulation (PAM), phase-shift keing (PSK), quadratude amplitude modulation (QAM) and amplitude phase shift keying (APSK).

### B. Discrete-time system model

To evaluate the performance of the AC hybrid FSK-based modulations, we built a discrete-time model for the communication system. Considering a sampling frequency $F_c = 1/T_c$, $T_c$ being the chip time with $T_c = T_s/N$ and $N = 4M_\perp$ the number of chips per symbol. The $k^{th}$ discrete time sample of AC hybrid FSK-based symbol is expressed as:

$$\forall k \in [\![0;N-1]\!],\ g_{m,i}[k] = \text{Clip}\left\{ A_i \cos\left( \frac{2\pi m k}{N} + \phi_i \right) \right\} \quad (2)$$

Fig. 1(a) shows an example of the available symbols for $M_\perp = 4$, $m = 1$, $A_i = 1$ and $\phi_i \in \{0, \frac{\pi}{2}, \pi, \frac{3\pi}{2}\}$. Examples of constellations for $M_L = 8$ are presented in Fig. 2.

The discrete-time AC hybrid FSK-based symbols defined in (2) can be obtained from inverse discrete Fourier transform (IDFT) of size $N = 4M_\perp$ for which the input is a FD vector $\boldsymbol{X_{m,i}}$, satisfying Hermitian symmetry, and expressed as:

$$\boldsymbol{X_{m,i}} = (0,...,0, \underbrace{A_i e^{j\phi_i}}_{X_{m,i}(m)}, 0,...,0, \underbrace{A_i e^{-j\phi_i}}_{X_{m,i}(N-m)}, 0,...,0) \quad (3)$$

Fig. 3 describes the transmission model. A sequence of $n$ bits, with $n = \log_2(M_\perp M_L)$ defines the frequency index $m$, amplitude $A_i$ and phase $\phi_i$ to generate $\boldsymbol{X_{m,i}}$. IDFT of $\boldsymbol{X_{m,i}}$ is realized through an inverse fast Fourier transform (IFFT) and the obtained time-domain signal is clipped to generate the AC hybrid FSK-based symbol. The waveform is sent in an additive white Gaussian noise (AWGN) channel with a bilateral PSD of $N_0/2$. The received signal $y$ is processed at receiver to retrieve the frequency, amplitude and phase and finally the $n$ bits sequence.

### C. Spectral efficiency

The spectral efficiency $\eta$, expressed in bits/s/Hz, is defined by:

$$\eta = \frac{R_b}{B}, \quad (4)$$

where $R_b$ is the bit rate (bits/s) and $B$ is the monolateral baseband bandwidth. Since $n = \log_2(M_\perp M_L)$ bits are sent per symbol during $T_s$, we get $R_b = \frac{\log_2(M_\perp M_L)}{T_s}$. If, as a first simplifying assumption, out-of-band harmonics due to clipping are neglected, $B = 2M_\perp \Delta f = \frac{2M_\perp}{T_s}$ and the expression for $\eta$ is:

$$\eta = \frac{\log_2(M_\perp M_L)}{2M_\perp}. \quad (5)$$

The spectral efficiency depends on the size of the dictionary $M = M_\perp M_L$ and not on the type of constellation used for the elementary symbols. Formula (5) is in agreement with [8] for the special case of PSK linear elementary symbols.

## III. WAVEFORM FREQUENCY-DOMAIN ANALYSIS AND HARMONIC RECEIVER

In [8], a FD harmonic receiver is proposed for AC $M_\perp$-FSK $M_L$-PSK. This receiver reaches the performance of the maximum likelihood (ML) receiver with a reduced complexity ($2M_\perp^2 M_L$ non-zero real multiplications for the ML receiver and $8M_\perp \log_2(4M_\perp) + 6M_\perp M_L$ for the harmonic receiver with three taps). However, it necessitates off-line computations of all FD waveforms of the dictionary. In this section, we propose a FD analysis of the AC hybrid FSK-based waveforms (generalized to all the considered linear modulation schemes) to derive theoretically the necessary FD components of the waveforms used in the harmonic receiver.

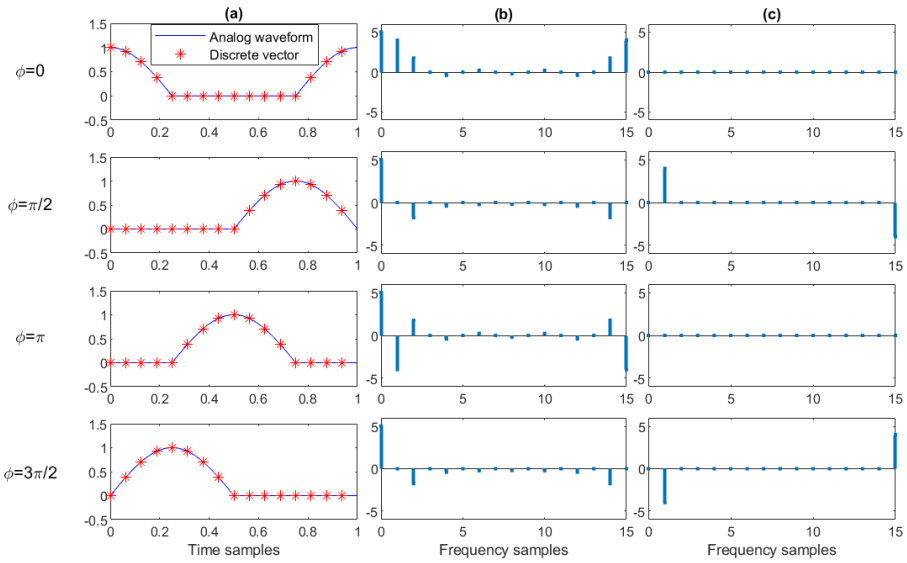


Fig. 1. (a) Analog and discrete time AC 4-FSK 4-PSK waveforms (b) Real part of the DFT (c) Imaginary part of the DFT for $m$=1, $A_i$=1 and $\phi_i \in \{0, \frac{\pi}{2}, \pi, \frac{3\pi}{2}\}$.

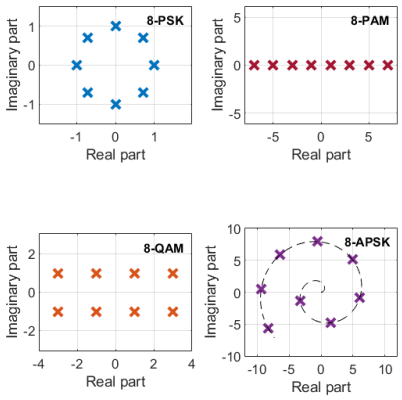


Fig. 2. Constellations for the linear part of the modulation for $M_L$=8.

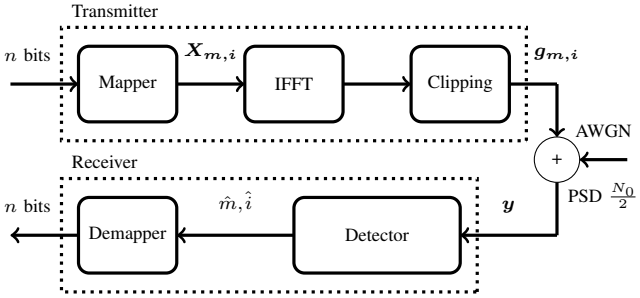


Fig. 3. Emission, channel model and reception.

### A. *Frequency-domain waveforms*

Let us denote $G_{m,i}$ the Fourier transform of the analog waveform $g_{m,i}$ defined in (1). If we define a function $f_{m,i}$ as $f_{m,i}(t)=\text{Clip}\left(A_i \cos\left(2\pi \frac{m}{T_s} t+\phi_i\right)\right)$, the frequency-domain waveform $G_{m,i}$ can be expressed as:

$$G_{m,i}(\nu)=\mathcal{F}_t\left[f_{m,i}(t)\right](\nu) * \mathcal{F}_t\left[\Pi_{[0;T_s[}(t)\right](\nu), \tag{6}$$

where $\mathcal{F}_t$ is the notation for the Fourier transform with respect to the variable $t$, $*$ refers to the convolution operation. $f_{m,i}$ is periodic of period $\frac{T_s}{m}$ and thus can be expressed as a Fourier series: $f_{m,i}(t)=\sum_{n=-\infty}^{+\infty} c_n e^{j2\pi \frac{nm}{T_s} t}$. Computing the Fourier coefficients $c_n$, at frequencies $\nu=nm/T_s$, one obtains:

$$\forall n \in \mathbb{Z}, \quad c_n = A_i \alpha_n e^{jn\phi_i}$$
$$\text{with } \alpha_n = \begin{cases} \frac{1}{4} & \text{if } n=1 \text{ or } n=-1 \\ \frac{1}{\pi(1-n^2)} \cos\left(\frac{\pi}{2} n\right) & \text{otherwise,} \end{cases} \tag{7}$$

such that (6) rewrites:

$$G_{m,i}(\nu)=A_i T_s \sum_{n=-\infty}^{+\infty} \alpha_n e^{jn\phi_i} e^{-j\pi\left(\nu-\frac{nm}{T_s}\right)T_s} \text{sinc}\left(\left(\nu-\frac{nm}{T_s}\right)T_s\right) \tag{8}$$

The sinc function is defined by $\text{sinc}(0)=1$ and, for $x \neq 0$, $\text{sinc}(x)=\frac{\sin(\pi x)}{\pi x}$. From (6) and (7), it can be seen that only the DC component ($n$=0), the fundamental odd frequency ($n$=1) and even harmonics of the fundamental (even values for $n$) are present in the FD waveform. This justifies the use of the frequency grid with only odd fundamental frequency indexes: no harmonic created by the clipping operation will fall on one of the fundamental components.

The discrete FD waveform (i.e. DFT of $g_{m,i}[k]$) $\boldsymbol{G_{m,i}}=[G_{m,i}[1],\cdots,G_{m,i}[N]]^{\mathrm{T}}$ can be derived from (8). The $l^{th}$ component $G_{m,i}[l]$ of the discrete FD waveform is given by:

$$G_{m,i}[l]=\frac{N}{T_s} \sum_{k=-\infty}^{+\infty} G_{m,i}\left(\frac{l-kN}{T_s}\right). \tag{9}$$

Fig. 1 (b) and (c) present the frequency-domain waveforms of AC 4-FSK 4-PSK modulation, for $m$=1, $A_i$=1 and $\phi_i$=0, $\pi$/2, $\pi$ and 3$\pi$/2.

Considering the fact that the coefficients $\alpha_n$ decay as $\frac{1}{n^2}$, an approximation of $\boldsymbol{G_{m,i}}$ can be deduced by neglecting $\alpha_n$ for $n>2$. Indeed, 99% of the signal energy is contained in the DC component, the fundamental and the first harmonic. Table I shows the values of $\alpha_n$ for $n$ ranging from 0 to 6. As a consequence, the discrete FD waveform can be simplified to an approximate version $\tilde{\boldsymbol{G}}_{\boldsymbol{m,i}}$ in which the only non-null components are $\tilde{G}_{m,i}[0]=\alpha_0 A$, $\tilde{G}_{m,i}[m]=\alpha_1 A_i e^{j\phi_i}$, $\tilde{G}_{m,i}[2m]=\alpha_2 A_i e^{j2\phi_i}$, $\tilde{G}_{m,i}[N-2m]=\alpha_2 A_i e^{-j2\phi_i}$ and $\tilde{G}_{m,i}[N-m]=\alpha_1 A_i e^{-j\phi_i}$.

TABLE I
FIRST VALUES OF $\alpha_n$

| $n$ | 0 | 1 | 2 | 3 | 4 | 5 | 6 |
|---|---|---|---|---|---|---|---|
| $\alpha_n$ | $\frac{1}{\pi}$ | $\frac{1}{4}$ | $\frac{1}{3\pi}$ | 0 | $-\frac{1}{15\pi}$ | 0 | $\frac{1}{35\pi}$ |

### B. Harmonic receiver implementation

In the harmonic receiver presented in [8], as a first step, a $N$-order DFT of the received signal $y$ is computed as:

$$\boldsymbol{Y}=\boldsymbol{F}\boldsymbol{y}, \tag{10}$$

where $\boldsymbol{F}$ is the $N$-order DFT matrix and $\boldsymbol{Y}=[Y[1],\cdots,Y[N]]^{\mathrm{T}}$. As a second step in [8], FD cross-correlations are realized between $\boldsymbol{Y}$ and pre-computed FD vectors, keeping only the fundamental and the first harmonic, to identify the transmitted symbol. Here, the DC component should also be considered, as the linear part of the modulation may concern not only the phase but also the amplitude. In this work, we propose to use the theoretically defined FD waveforms $\tilde{\boldsymbol{G}}_{\boldsymbol{m,i}}$, to avoid any off-line computation. As a result, the estimated symbol indices $\hat{i}$ and $\hat{m}$ can be identified directly through frequency-domain cross-correlations as:

$$\begin{aligned}\hat{m},\hat{i}=&\arg\max_{m,i}\langle\boldsymbol{Y},\tilde{\boldsymbol{G}}_{\boldsymbol{m,i}}\rangle-\frac{1}{2}\|\tilde{\boldsymbol{G}}_{\boldsymbol{m,i}}\|^2\\ &\text{with}\ \begin{matrix}m\in\{1,3,\cdots,2M_\perp-1\}\\ i\in\{0,1,\cdots,M_L-1\}\end{matrix}\\ \text{and}\ \langle\boldsymbol{X},\boldsymbol{Y}\rangle=&\Re\left(\boldsymbol{X}^{\mathrm{T}}\boldsymbol{Y}^{*}\right)\ \text{and}\ \|\boldsymbol{X}\|=\sqrt{\langle\boldsymbol{X},\boldsymbol{X}\rangle}.\end{aligned} \tag{11}$$

In the case of PSK constellations, all waveforms have the same energy and the term in $\|\tilde{\boldsymbol{G}}_{\boldsymbol{m,i}}\|^2$ can be omitted in (11). Fig. 4 presents the model of the harmonic receiver. According to [8], the performance of the harmonic receiver is quasi equivalent to the maximum likelihood (ML) receiver, obtained by replacing $\tilde{\boldsymbol{G}}_{\boldsymbol{m,i}}$ with $\boldsymbol{G}_{\boldsymbol{m,i}}$ in (11). A natural sub-optimal receiver in [8] (one-tap DFT receiver), renamed here fundamental component receiver, uses only odd frequencies, with decisions based only on the detection of the fundamental component and not on the harmonics generated by the non-linear clipping process, with a reduced complexity of $8M_\perp\log_2(4M_\perp)+4M_L$ non-zero real multiplications.

## IV. Simulation results

Fig. 5 shows the simulation results for the bit error rate (BER) of AC 16-FSK 4-PSK as a function of $E_b/N_0$, $E_b$ being the average energy per bit. From Fig. 5, it can be seen that the theoretical FD waveforms used in the proposed harmonic receiver implementation lead to similar BER results as for the ML receiver, without the need for off-line FD waveforms pre-computation. Fig. 6 presents the simulation results for the spectral efficiency as a function of the required $E_b/N_0$ to reach a BER of $10^{-3}$, for different AC hybrid FSK-based

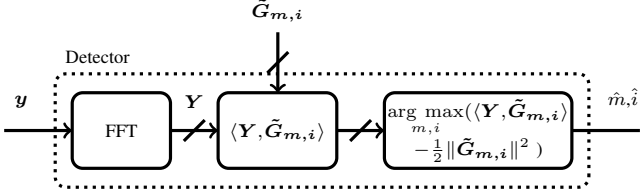


Fig. 4. Harmonic receiver model

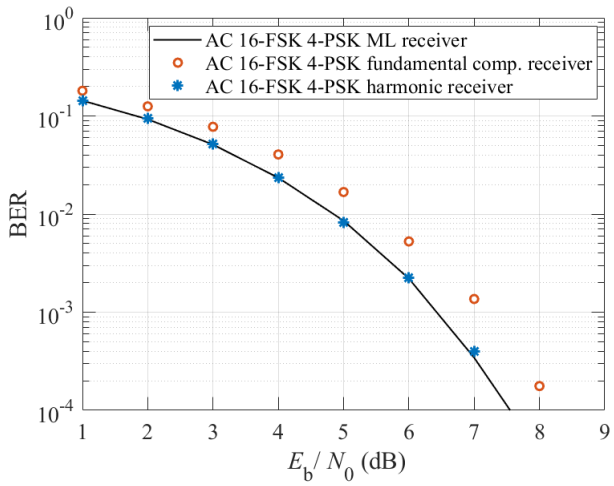


Fig. 5. Binary error rate for an AC 16-FSK 4-PSK modulation, versus $E_b/N_0$.

modulations, considering the aforementioned linear modulation schemes. Harmonic receiver is used. As it can be observed from Fig. 6, the best trade-off between spectral efficiency and energy efficiency is obtained for AC $M_\perp$-FSK 4-PSK and AC $M_\perp$-FSK 8-PSK modulations. Since phase modulation does not cause any change in the DC component, DC can be omitted in $\tilde{\boldsymbol{G}}_{\boldsymbol{m,i}}$, reducing the harmonic receiver complexity. Moreover, it is known that, for VLC applications, detection of the DC can be corrupted by the ambient noise [12]. Also, in Fig. 6, it is visible that higher orders $M_L$ for AC $M_\perp$-FSK $M_L$-QAM ($M_L$>4) and AC $M_\perp$-FSK $M_L$-PSK ($M_L$>16) are strongly impacted by the reduced Euclidean distance between the symbols: while energy efficiency is heavily penalized, the gain in spectral efficiency is insufficient. AC $M_\perp$-FSK $M_L$-PAM and AC $M_\perp$-FSK $M_L$-APSK modulations show degraded performance even for low $M_L$ values still due to the reduced Euclidean distance between the symbols. In Fig. 6, the simulation results are benchmarked with conventional OOK, 4-PAM [3] and asymmetrically clipped optical OFDM (ACO-OFDM) [4] used in VLC applications. It is obvious that AC $M_\perp$-FSK 4-PSK and AC $M_\perp$-FSK 8-PSK modulations offer a large gain in energy efficiency relatively to ACO-OFDM and $M$-PAM, at the expense of spectral efficiency. Typical use cases of AC $M_\perp$-FSK 4-PSK and AC $M_\perp$-FSK 8-PSK modulations are low data rate wireless communications for VLC or RF communications with envelope detection, for which the spectral efficiency penalty would not be a strong limitation.

## V. Power spectral density of AC hybrid FSK-based modulations

The confidence in the performance evaluation of AC hybrid FSK-based modulations relies on a correct definition of the spectral efficiency. Our first evaluation of the bandwidth $B$, in section II, was made by neglecting the out-of-band harmonics as a simplifying hypothesis. However, it is necessary to investigate the power spectral density (PSD) of AC hybrid

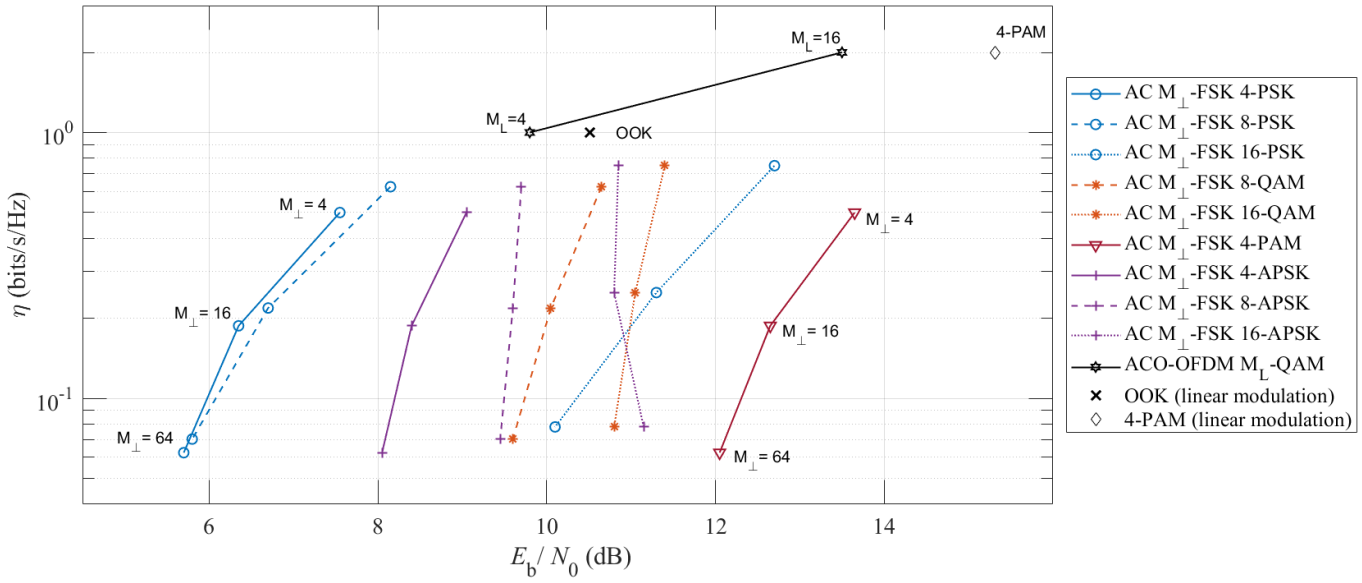


Fig. 6. Spectral efficiency versus $E_b/N_0$ for a BER of $10^{-3}$. Results obtained for 4, 16 and 64 carriers in the case of an AC hybrid FSK-based modulation with different constellations. 4-PSK and 4-QAM constellations differ by only a phase shift and result in the same performance. Modulations based on PAM constellations for $M_L \geq 8$ require $E_b/N_0 > 16$ and are not mentioned on the figure. Benchmark comparison with OOK [8], PAM [5] and ACO-OFDM [8].

FSK-based modulations to provide accurate evaluations for $B$ and related spectral efficiency.

### A. General formula for the PSD

The sent signal is a serial transmission of an infinity of AC hybrid FSK-based symbols. According to [11], its PSD is written as $\Gamma(\nu)=\Gamma_d(\nu)+\Gamma_c(\nu)$ with:

$$\Gamma_d(\nu)=\frac{1}{M^2T_s^2}\sum_{l=-\infty}^{+\infty}\left|\sum_{m,i}G_{m,i}\left(\frac{l}{T_s}\right)\right|^2\delta\left(\nu-\frac{l}{T_s}\right)$$

and

$$\Gamma_c(\nu)=\frac{1}{T_s}\left[\sum_{m,i}\frac{1}{M}|G_{m,i}(\nu)|^2-\left|\sum_{m,i}\frac{1}{M}G_{m,i}(\nu)\right|^2\right], \quad (12)$$

where $G_{m,i}(.)$ expressed in (8) are the Fourier transforms of the analog waveforms. $\Gamma(\nu)$ includes a spectral line part $\Gamma_d(\nu)$ and a continuous part $\Gamma_c(\nu)$.

### B. Approximated closed-form PSD for AC $M_\perp$-FSK $M_L$-PSK

In the following, we limit the PSD analytical study to AC $M_\perp$-FSK $M_L$-PSK, for which the best spectral efficiency vs energy efficiency trade-off has been obtained in section IV. For $i\in\{0,...,M_L-1\}$, the $M_L$ elementary symbols are defined as:

$$A_i=1 \text{ and } \phi_i=2\pi i/M_L. \quad (13)$$

It is possible to obtain a closed-form expression for the PSD, by means of an approximation for $\Gamma_c(\nu)$: in the expression (8) of $G_{m,i}$, only the terms related to $\alpha_0$, $\alpha_{\pm1}$ and $\alpha_{\pm2}$ are kept. For $\Gamma_d(\nu)$, no approximation is needed. It can be shown after some manipulations that, for $\nu\in\mathbb{R}$:

$$\Gamma_c(\nu)\approx\frac{T_s}{M_\perp\pi^2}\sum_{p=0}^{M_\perp-1}\frac{4\nu^2T_s^2\text{sinc}^2(|\nu|T_s-2(2p+1))}{9(|\nu|T_s+2(2p+1))^2}+\frac{\pi^2\left(\nu^2T_s^2+(2p+1)^2\right)\text{sinc}^2(|\nu|T_s-(2p+1))}{8(|\nu|T_s+(2p+1))^2} \quad (14)$$

and with $\Omega_l=\{k\in\mathbb{Z},\ \exists p\in[\![0;M_\perp-1]\!],\ l=k(2p+1)\}$:

$$\Gamma_d(\nu)=\frac{1}{M_\perp^2}\sum_{l=-\infty}^{+\infty}\left|\sum_{k\in\Omega_l}\alpha_k\right|^2\delta\left(\nu-l\frac{M_L}{T_s}\right). \quad (15)$$

In (15), the coefficients $\alpha_k$ are those defined in (7). Fig. 7 presents an example of the PSD for a modulation AC 4-FSK 4-PSK, and compares the theory with a Monte Carlo estimation. The frequency is normalized by $B=\frac{2M_\perp}{T_s}$, so we expect spectral lines at frequencies $\nu=l\frac{B}{2}$, $l\in\mathbb{Z}$.

We can make the approximation that almost all the power of the spectral line part is contained in the DC component, of numerical value $\frac{1}{\pi}$. Knowing that the total power of the signal is $\frac{1}{4}$, it means that around 60% of the power is contained in the continuous part and 40% in the discrete part, and more specifically here in the DC component.

### C. Revision of spectral efficiency evaluation

Considering the previous power spectral density results, it appears that the occupied bandwidth can not be evaluated only on the basis of fundamental frequencies as in [8]. Thus, we define an out-of-band parameter $\beta$ such as 99% of the signal power is in the frequency band $[-(1+\beta)B;(1+\beta)B]$. Simulations were made for $M_\perp$ between 4 and 64 and $M_L$

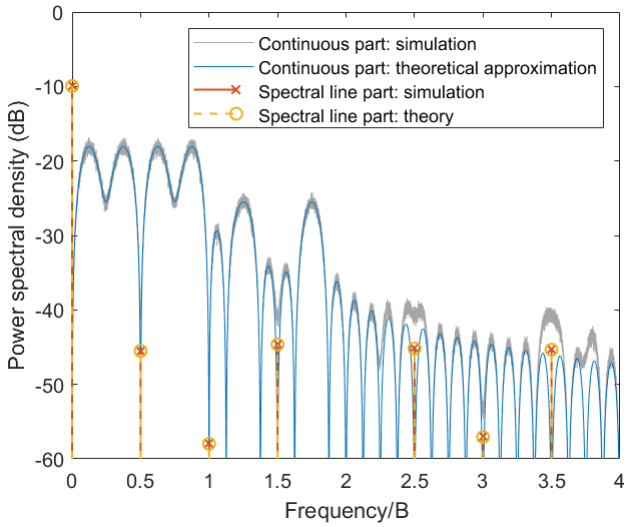


Fig. 7. PSD of AC 4-FSK 4-PSK.

between 4 and 32, and $\beta$ is found to be around 0.9. This means that the bandwidth of the analog signal is almost twice as big as the one obtained considering only the fundamental frequencies [8] leading to a penalty on spectral efficiency.

Fig. 8 shows an update of the performance results for spectral efficiency versus energy efficiency, taking into account the bandwidth occupied by the analog signal, assuming the same target BER of $10^{-3}$. We focused only on the most efficient techniques, which are AC $M_{\perp}$-FSK $M_L$-PSK modulations with $M_L$ not greater than 16. Even considering the aforementioned correction on spectral efficiency, the performance of AC $M_{\perp}$-FSK 4-PSK and AC $M_{\perp}$-FSK 8-PSK modulations outperforms other conventional schemes for applications addressing low data rate wireless communications.

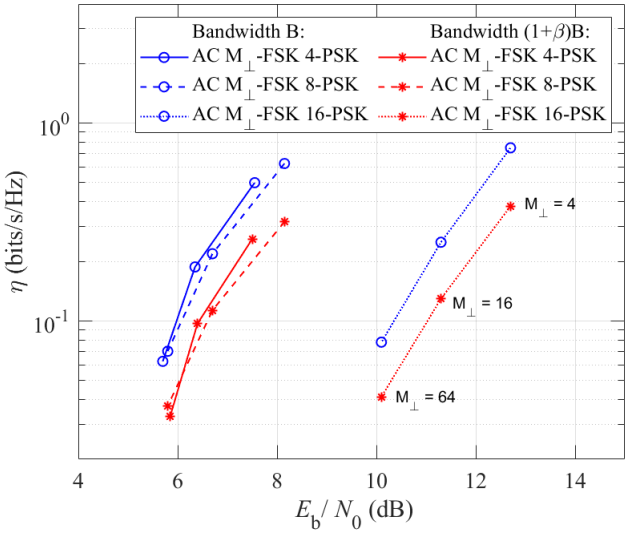


Fig. 8. Spectral efficiency as a function of energy efficiency for a BER of $10^{-3}$ and AC $M_{\perp}$-FSK $M_L$-PSK modulations, with $M_{\perp} \in \{4,16,64\}$. Comparison with the corrected version of the spectral efficiency, taking into account out-of-band harmonics.

## VI. Conclusion

In this paper, unipolar AC hybrid FSK-based modulations are studied, comparing different possible linear (phase/amplitude) modulations. This work highlights that this hybrid modulation with 4-PSK and 8-PSK alphabets reaches the best energy efficiency/spectral efficiency trade-off over alternatives, including conventional $M$-PAM and ACO-OFDM modulations. Closed-form expressions of dictionary waveforms in frequency-domain justify the use of odd frequencies from the original $2M_{\perp}$-FSK and have been introduced in a low complexity harmonic receiver to achieve similar performance as the maximum likelihood receiver, without the need of any off-line computation. Finally, a closed-form expression of the power spectral density of AC $M_{\perp}$-FSK $M_L$-PSK has been evaluated and leads to a more relevant definition for the signal bandwidth and spectral efficiency. A perspective of this work may include a study of AC hybrid FSK-based modulations in a more realistic frequency-selective channel and an extension to a dual-tone modulation scenario.

## References


[1] A. Celik, I. Romdhane, G. Kaddoum, and A. M. Eltawil, "A top-down survey on optical wireless communications for the internet of things," *IEEE Comm. Surveys & Tutorials*, vol. 25, no. 1, pp. 1–45, 2023.

[2] N. J. Estes, X. Kang, X. Meng, *et al.*, "A 0.71-mW antenna-coupled on–off-key receiver for Gbps millimeter-wave wireless communications," *IEEE Transactions on Microwave Theory and Techniques*, vol. 71, no. 4, pp. 1793–1808, 2023.

[3] M.-A. Khalighi, S. Long, S. Bourennane, and Z. Ghassemlooy, "PAM- and CAP-based transmission schemes for visible-light communications," *IEEE Access*, vol. 5, pp. 27 002–27 013, 2017.

[4] S. Ma, R. Yang, X. Deng, *et al.*, "Spectral and energy efficiency of ACO-OFDM in visible light communication systems," *IEEE Transactions on Wireless Communications*, vol. 21, no. 4, pp. 2147–2161, 2022.

[5] J. G. Proakis and M. Salehi, *Digital communications*. McGraw-Hill., 2008.

[6] C. Manimegalai, S. Gauni, N. Raghavan, and T. R. Rao, "Investigations on suitable modulation techniques for visible light communications," in *2017 International Conference on Wireless Communications, Signal Processing and Networking (WiSPNET)*, IEEE, 2017, pp. 1818–1822.

[7] G. M. Yamga, A. R. Ndjiongue, and K. Ouahada, "Low complexity clipped frequency shift keying (FSK) for visible light communications," in *2018 IEEE 7th International Conference on Adaptive Science & Technology (ICAST)*, 2018, pp. 1–6.

[8] M. J. Khan, A. W. Azim, Y. Le Guennec, G. Maury, and L. Ros, "AC-FPSK modulation for low-energy and low data rate optical wireless communications," *AEU - International Journal of Electronics and Communications*, vol. 178, p. 155 243, 2024.

[9] R. A. Khalona, G. E. Atkin, and J. L. LoCicero, "On the performance of a hybrid frequency and phase-shift keying modulation technique," *IEEE Transactions on Communications*, vol. 41, no. 5, pp. 655–659, 1993.

[10] Y. Roth, J-B. Doré, L. Ros, and V. Berg, "Coplanar Turbo-FSK: A Flexible and Power Efficient Modulation for the Internet-of-Things," *Wireless Communications and Mobile Computing*, 2018.

[11] S. G. Wilson, *Digital Modualtion and Coding*. Pearson, 1995.

[12] T. Adiono, S. Fuada, "Optical interference noise filtering over visible light communication system utilizing analog high-pass filter circuit," *Proc. of the 2017 Int. Symp. on Nonlinear Theory and Its Applications*, pp. 616-619, 2017.